https://doi.org/10.5194/egusphere-2026-2253
Preprint. Discussion started: 27 May 2026

Advancing the Scenario-to-Climate Link with Spatial Emulators in the FASTMIP Pilot Experiment

Michael G. Windisch1, Yann Quilcaille1, Camilla Mathison2,3, Claudia Tebaldi4, Eleanor Burke2, Laila Gohar2, Chris Smith5, Sarah Schöngart1, Abigail Snyder4, Siddarth Durga4, Kalyn Dorheim4, and Sonia I. Seneviratne1

1 Institute for Atmospheric and Climate Science, Department of Environmental Systems Science, ETH Zurich.
2 Met Office Hadley Centre, Exeter, UK
3 School of Geography, University of Leeds, UK
4 University of Maryland College Park, MD, USA
5 Energy, Climate and Environment Program, International Institute for Applied Systems Analysis (IIASA), Laxenburg, Austria

Correspondence to: Michael G. Windisch [michael.windisch@env.ethz.ch]

Abstract.

Creating internally consistent climate scenarios remains a challenge in climate research. While Earth System Models (ESMs) offer detailed regional outcomes able to resolve and discover physical dynamics and drivers, their computational cost prevents them from covering the full range of emissions and land-use scenarios produced by Integrated Assessment Models (IAMs). As a result, the modelling chain from IAMs through Simple Climate Models (SCMs) to ESMs informing climate change assessments remains limited in its full deployment to a handful of scenarios, leaving most IAM scenarios lacking their corresponding regional climate information and limiting our ability to assess their implications for local impacts. This modelling chain also remains largely unidirectional: Climate outcomes are seldom fed back to inform the underlying scenarios whose development therefore may miss important potential feedback between physical climate and socioeconomic futures. Here, we introduce FASTMIP (Fast Assessment for Scenario Trajectories Multi-emulator Intercomparison Project), a coordinated effort to rapidly translate socioeconomic scenarios into spatial climate outcomes using emulators. In this FASTMIP pilot experiment, we apply three spatial emulators (MESMER, PRIME, and STITCHES) to a shared set of scenarios that includes both widely used CMIP6 pathways and scenarios without dedicated ESM simulations. The results show how spatial emulation could provide information on climate feedback to constrain scenario assumptions, extend scenario-to-climate coverage, support regionally differentiated assessments, and therefore reveal current limitations in the climate projection pipeline that limit a more comprehensive linkage and evaluation of scenario-to-climate outcomes. We show that for these 3 emulators there is consistency in the results, particularly for the center of the distribution. Addressing the limitations identified here at the scenario-to-climate interface could enable spatial emulators to systematically deliver rapid regional insights and support more consistent climate scenario development in future coordinated IAM-ESM modelling exercises.

https://doi.org/10.5194/egusphere-2026-2253
Preprint. Discussion started: 27 May 2026

1 Introduction

Climate projections require integrating trajectories of human activity with the physics of the climate system. This task is divided between different model families: Integrated Assessment Models (IAMs) explore socio-economic futures and generate emissions and land use scenarios and Earth System Models (ESMs) simulate physically consistent, gridded climate responses using a subset of these pathways as external forcings, forming a scenario-to-climate link (van Vuuren et al., 2025). However, the computational cost of ESMs constrains both the number of scenarios and the ensemble size that can be explored. As a result, only a small fraction of future scenarios created by IAMs are run by ESMs, and even fewer are simulated across a large ensemble of models or realizations of the same model (Eyring et al., 2016; Tebaldi et al., 2021; van Vuuren et al., 2025).

In parallel, Simple Climate Models (SCMs) calibrated on ESMs translate more of these pathways into climate projections, but are limited by their temporal and spatial resolution and often only able to provide global annual mean temperature and sea-level rise pathways. SCMs are also used to provide concentration timeseries of greenhouse gases for ESMs, when they do not have the capability to run in emissions-driven mode (Romero-Prieto et al., 2026; Smith and Gasser, 2022).

As a result, most future socio-economic pathways and their associated emission and land-use scenarios lack regional climate information, limiting systematic exploration of the scenario-to-climate space and constraining probabilistic climate impact assessments because the few scenarios with ESM output often rely on small ensemble sizes. In addition, the modelling chain from IAMs to SCMs and ESMs remains largely one-directional, where spatial climate outcomes are seldom fed back to constrain the assumptions underlying scenario development (Kikstra et al., 2022; Riahi et al., 2017; Tebaldi et al., 2021; van Vuuren et al., 2025). Recent work has begun to improve on these limitations by starting to integrate climate and human systems (Calvin and Bond-Lamberty, 2018; Collins et al., 2015; Hartin et al., 2021; Schoenberg et al., 2025; Di Vittorio et al., 2025).

Spatial climate emulators, once trained, are computationally much cheaper than ESMs and can rapidly provide gridded climate outcomes for a much broader range of scenarios than currently covered by ESM simulations. They also provide the ability to generate many realizations to better sample the probability distribution generated by internal variability of variables of interest, including the tails of those climate distributions for climate impact assessments (Tebaldi et al., 2025). Trained on ESM output but taking SCM projections as input, most of these emulators generate gridded responses conditioned on global-mean temperatures, producing gridded climate and exposure metrics at a fraction of the computational cost.

Here, we introduce the FASTMIP (Fast Assessment for Scenario Trajectories Multi-emulator Intercomparison Project) pilot experiment, a coordinated effort to accelerate the translation of socioeconomic scenarios into spatial climate outcomes using emulators. In this first FASTMIP effort, three spatial ESM emulators are applied to a set of existing scenarios that includes both widely used pathways (in the form of the main scenarios run by the Coupled Model Intercomparison Project, Phase 6 (CMIP6) and assessed in the AR6 WG1 report), referred to from hereon as CMIP6 scenarios (Riahi et al., 2017) and scenarios for which no ESM simulations exist (developed within the Network for the Greening of the Financial System

https://doi.org/10.5194/egusphere-2026-2253
Preprint. Discussion started: 27 May 2026

(NGFS) project) (Richters et al., 2024). To this end, we combine inputs from SCMs and IAMs with three spatial ESM emulators trained on ESMs' output available through the CMIP6 archive (MESMER (Beusch et al., 2020; Quilcaille et al., 2023), PRIME (Mathison et al., 2025), and STITCHES (Tebaldi et al., 2022)) and produce ensembles of climate outcomes.

The FASTMIP pilot allows for the exploration of the potential of spatial emulators to accelerate the scenario-to-climate link (Sect. 2) and illustrates the potential benefits of this faster link (Sect. 3) by showcasing potential constraints on scenario mitigation assumptions that could emerge if climate impacts were fed back into scenario development (Sect. 3.1), populating the scenario-to-climate whitespace (Sect. 3.2), addressing underexplored regional heterogeneity (Sect. 3.3), exploring previously unquantified scenario-to-climate outcomes (Sect. 3.4), and looking into the drivers of uncertainty in emulated regional outcomes (Sect. 4).

By providing common inputs, a shared experimental design, and publicly archiving all emulator outputs, the FASTMIP pilot experiment enables other emulators to reproduce the experiment and compare results. A similar coordinated effort could potentially be replicated to rapidly provide initial, regional insights into the forthcoming CMIP7 generation of ScenarioMIP pathways intended to supersede the CMIP6 scenarios (van Vuuren et al., 2025).

2 Accelerating the scenario-to-climate link

Spatial emulators offer a way to accelerate the connection between scenario development and regional climate information, addressing a bottleneck in the current scenario-to-climate modelling chain (Kikstra et al., 2022; Tebaldi et al., 2025). FASTMIP builds on this capability by coordinating spatial emulators using shared inputs and a common experimental setup. This coordinated approach enables a low computational-cost scenario-to-climate link that can support both unidirectional analysis, in which scenario-to-climate outcomes are the endpoint or used as input to impact assessment (here termed exogenous analyses), and iterative analyses, in which the scenario-to-climate outcomes feed back into scenario development and help constrain scenario assumptions (here termed endogenous analyses).

In this study, we implement the FASTMIP pilot experiment by coordinating three spatial emulators, MESMER, PRIME, and STITCHES, using a shared experimental setup (Figure 1). We build on existing emissions pathways from IAMs and their translation into probabilistic global mean temperature trajectories using SCMs, a step that is already routinely embedded in scenario development. Ensuring the use of consistent SCM-derived temperature trajectory inputs to the emulators based on the specific combinations of scenario, IAM, SCM, and probabilistic SCM outcomes enables direct comparison across scenarios and uncertainty sources.

Each emulator is trained on output from CMIP6 ESMs and translates global mean temperature change into spatially explicit climate responses. The experiment spans both well-established pathways with dedicated ESM simulations, namely the CMIP6 scenarios (Riahi et al., 2017), and scenarios without dedicated ESM output developed by the NGFS (Richters et al., 2024). Further details of the experimental design and the individual emulators are provided in the Methods section.

https://doi.org/10.5194/egusphere-2026-2253
Preprint. Discussion started: 27 May 2026

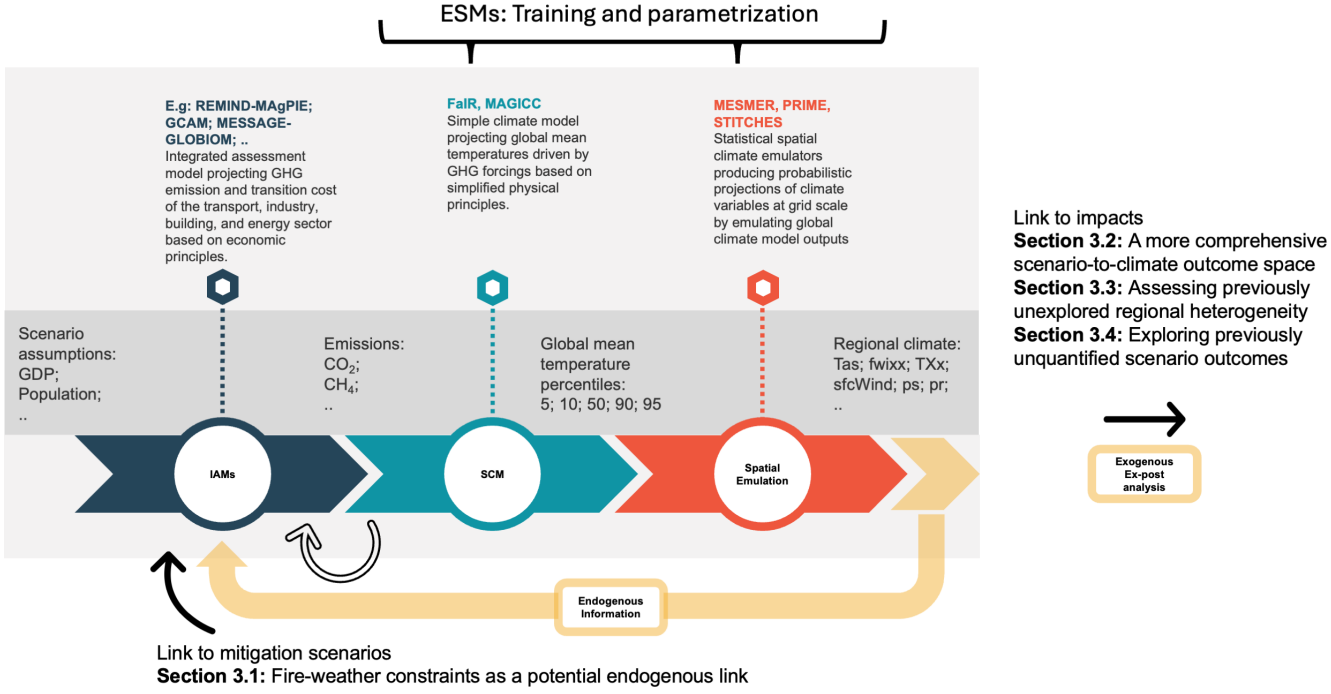

Figure 1. Scenario-to-spatial-climate workflow. IAMs (dark blue) produce emissions and socioeconomic trajectories; SCMs (teal) provide probabilistic global temperature pathways; spatial emulators (red) generate gridded climate outcomes and derived exposure metrics. Yellow indicates two potential use cases for the regional climate outcomes: exogenous analyses (informing impact and adaptation assessments) and endogenous analyses (providing feedback to IAMs).

The resulting spatial climate outcomes can be used in two complementary ways. First, they enable exogenous analyses, in which spatial climate information is used to assess the implications of scenarios, such as climate impacts, adaptation needs, or comparative assessments, without altering the scenario assumptions themselves. Exogenous analyses can help to fill gaps in the scenario-to-climate space by placing the climate implications of additional emission pathways in the context of the handful of scenarios that were run by ESMs (Sect. 3.2, Figure 3) and by enabling early-stage assessments relevant for impact and adaptation studies (Sect. 3.3 & 3.4, Figure 4 & 5).

Second, the spatial climate outcomes open the door to endogenous analyses, in which spatial climate information informs or constrains scenario development by feeding information back into IAMs. In principle, such feedback could make scenario assumptions more plausible and internally consistent with their own projected climate reality by accounting for climate-driven constraints on mitigation options, energy demand, or land and water use. Examples include adjusting the deployment of bioenergy or reforestation, accounting for regional changes in heating and cooling degree days, changing assumptions about labour productivity as an impact of heat stress, or modifying water-use assumptions under altered hydrological regimes (Calvin and Bond-Lamberty, 2018; Dasgupta et al., 2021; Hartin et al., 2021; Hejazi et al., 2014; Jäger et al., 2024).

https://doi.org/10.5194/egusphere-2026-2253
Preprint. Discussion started: 27 May 2026

While such feedback are not yet implemented in most IAMs, they illustrate the potential for closer coupling between physical climate projections and socioeconomic modelling. An example explored within this experimental setup is presented in Section 3.1, where emulator-derived fire-weather indicators are combined with spatially explicit land-use projections to identify reforestation areas with increased fire-weather conditions. This example builds on previous analyses by Jaeger et al. (Jäger et al., 2024), indicating that "misplaced" reforestation commonly increases fire weather risk in addition to climate change, highlighting feedback that could be considered in future iterations of scenario design.

However, realizing endogenous feedback in practice crucially depend on the most widely used IAMs in scenario assessments being able to respond to spatial climate information. This may not always require gridded inputs, but at least derived indicators aggregated to spatial units meaningful to the model (e.g., countries or regions) or metrics based on climate thresholds such as masks, e.g. indicating where reforestation effectiveness would be limited by high fire weather occurrence. For much potential feedback, the barrier lies not only in providing spatial information itself, but in translating it into quantities compatible with the IAM's optimization process. Within this limitation, hazard-based indicators offer an intermediate step by identifying climate-driven constraints on mitigation options and enabling scenario variants that test the robustness and internal consistency of mitigation pathways derived by IAMs (Section 3.1).

Similarly, exogenous analyses benefit from socioeconomic data that are sufficiently spatially disaggregated. If such data are available, regional climate outcomes can be linked with the socioeconomic conditions where they matter most. For example, by combining spatial population or crop production data with spatial temperature and precipitation extremes to evaluate potential heat or drought exposure.

Currently, however, the publicly available data from IAMs, for instance via the IIASA Scenario Database (Byers et al., 2022.), limit such analyses. Many key variables are provided only at global or IAM-native super-region scales, limiting their use in spatially explicit assessments. Exceptions include the CMIP6 scenarios, for which gridded and harmonized land-use data exist via LUH2 (Hurtt et al., 2011), and the NGFS scenarios, which provide country-level socioeconomic outputs up to 2050 (Richters et al., 2024.).

3 Potential benefits of a fast scenario-to-climate link

In the following, we demonstrate the potential benefits of this accelerated workflow by applying it across a diverse set of socioeconomic pathways and assessments. The examples presented illustrate how rapid access to spatially explicit climate information can expand the explored scenario-to-climate space, reveal regionally differentiated outcomes, and support both exogenous assessment and exploratory endogenous constraints. Each subsection focuses on a distinct insight enabled by spatial emulation, highlighting aspects of scenario evaluation that were previously inaccessible for most scenarios caused by the ESM acting as bottleneck for spatial climate outcomes. All results shown in the following subsections are derived from spatially emulated climate outcomes applied consistently across scenarios.

https://doi.org/10.5194/egusphere-2026-2253
Preprint. Discussion started: 27 May 2026

3.1 Fire-weather constraints as a potential endogenous link

Storing carbon in forests is a key mitigation strategy in many IAM pathways(Popp et al., 2017; Riahi et al., 2017). However, IAMs frequently position future reforestation in areas that experience higher fire-weather conditions than existing forests (Jäger et al., 2024). Such "misplacement" introduces an elevated risk of fire-related carbon losses that remains unaccounted for in IAM-based climate change mitigation pathways.

Figure 2 illustrates how spatial emulators can reveal inconsistencies in IAM mitigation pathways by emulating future fire-weather hazards and intersecting them with land-use plans. The analysis shows that 44 % of forest expansion in SSP1-26 is allocated to regions where projected fire-weather conditions exceed the global mean experienced by existing forests in 2100, suggesting that a substantial fraction of planned sequestration may face elevated risk of fire-driven carbon loss.

Moreover, the highly skewed distribution of added fire-weather exposure (Figure 2c) indicates that a relatively small subset of candidate reforestation areas dominates cumulative exposure. In SSP1-26, the top 10 % of added tree-cover area accounts for roughly one-third (32.2 %) of cumulative added exposure, and half of the total added exposure is concentrated in only 20.7 % of the newly forested area. From an IAM perspective, this implies that modest reallocations of land could substantially reduce fire hazard associated with afforestation and reforestation measures.

Such emulated gridded hazard indicators offer a starting point for establishing endogenous links to feed back regional climate hazards into IAMs during scenario generation. Currently, however, the emulated fire-weather exposure presented here does not directly translate into expected carbon losses. As a result, the elevated future fire-weather conditions cannot directly affect the expected carbon content of forests within IAMs and, thus, do not yet have a direct link to the IAMs optimization, e.g. through an expected carbon price and assumed sequestration.

Until this structural gap between climate exposure and expected impact is overcome, spatial emulators could provide a first, enabling step. By identifying where mitigation pathways rely on land-use allocations that are systematically exposed to elevated future fire-weather conditions, emulator-derived hazard metrics allow the exploration of alternative scenarios through spatial constraints or penalty implementations.

For example, the scenario space that progressively avoids the most fire-exposed fractions of planned forest expansion (e.g. excluding the top 10 %, 20 %, one-third, or half of cumulative fire-weather exposure as illustrated in Fig. 2c) could be explored to assess how IAM optimization responds in terms of land allocation, mitigation costs, and competition between forestation and other mitigation options. Such constraints could be implemented analogue to existing land-protection schemes. In the absence of directly emulating carbon loss, a hazard-based approach could still provide a systematic way to probe the robustness and internal consistency of land-based mitigation pathways under climate-driven risk.

https://doi.org/10.5194/egusphere-2026-2253
Preprint. Discussion started: 27 May 2026

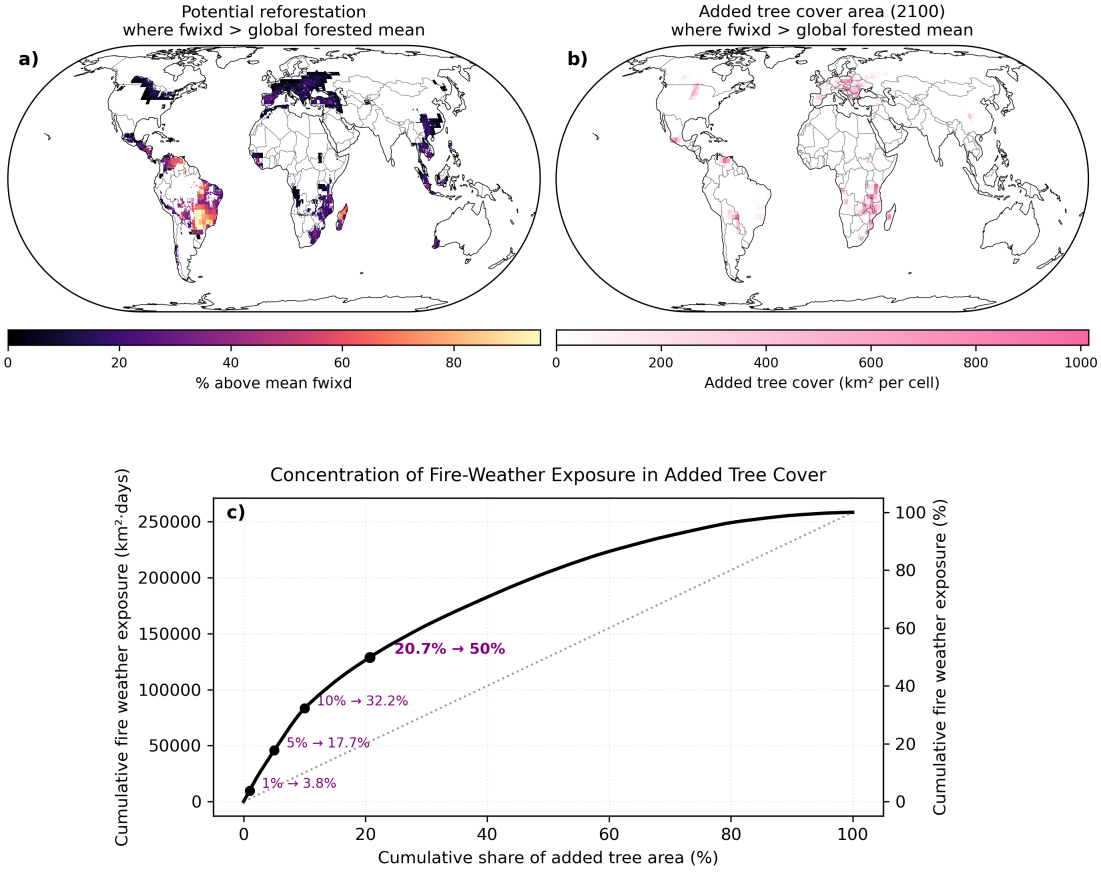

Figure 2: Emulated fire-weather conditions under SSP1-26. a) 2100 potential reforestation (pasture and cropland) areas where end-of-century SSP1-26 emulated extreme fire-weather index days (fwixd) exceed global mean fwixd over established forests, expressed as the percentage above this mean. b) Added tree cover area in SSP1-26 where fwixd exceeds the global forested mean. c) Concentration of cumulated fire-weather exposure times added tree cover (km2 times fwixd days). The dotted line marks the linear relationship between the cumulative share of added tree area to the cumulative fire weather exposure. The black line shows the relation under SSP1-26. Markers highlight selected percentiles showing the points (left) of the cumulative share of added tree area to (right) share of the cumulative fire weather exposure.

3.2 A more comprehensive scenario-to-climate outcome space

Although the widely used CMIP6 scenarios span diverse socioeconomic narratives, their realized emissions dynamics and associated climate exposure outcomes occupy a relatively constrained region of the scenario-to-climate outcome space (Figure 3). This limits the range of futures for which spatial climate outcomes can be systematically assessed and compared, as the majority of additional IAM scenarios lack any spatial climate outcomes.

Large regions of the scenario-to-climate outcome space therefore remain unexplored. In particular, combinations of emissions pathway dynamics and heat-exposure outcomes perpendicular to the main SSP axis are under-sampled. These gaps correspond to scenario outcomes with relatively slower emission declines and lower heat-exposure burdens above the SSP axis and outcomes with sharper emissions reductions associated with higher levels of heat exposure below the SSP axis.

https://doi.org/10.5194/egusphere-2026-2253
Preprint. Discussion started: 27 May 2026

The inclusion of NGFS scenarios by means of spatial emulation begins to populate this previously unquantified "scenario whitespace." The NGFS ensemble contributes several scenarios toward combinations of steeper emissions declines and higher heat-exposure outcomes, thereby extending the range of scenario-to-climate outcomes available for assessment (triangular markers in Figure 3). This demonstrates how emulated spatial climate outcomes can enable different scenario families to be compared within a common quantitative framework and how additional scenario sets can complement established pathways.

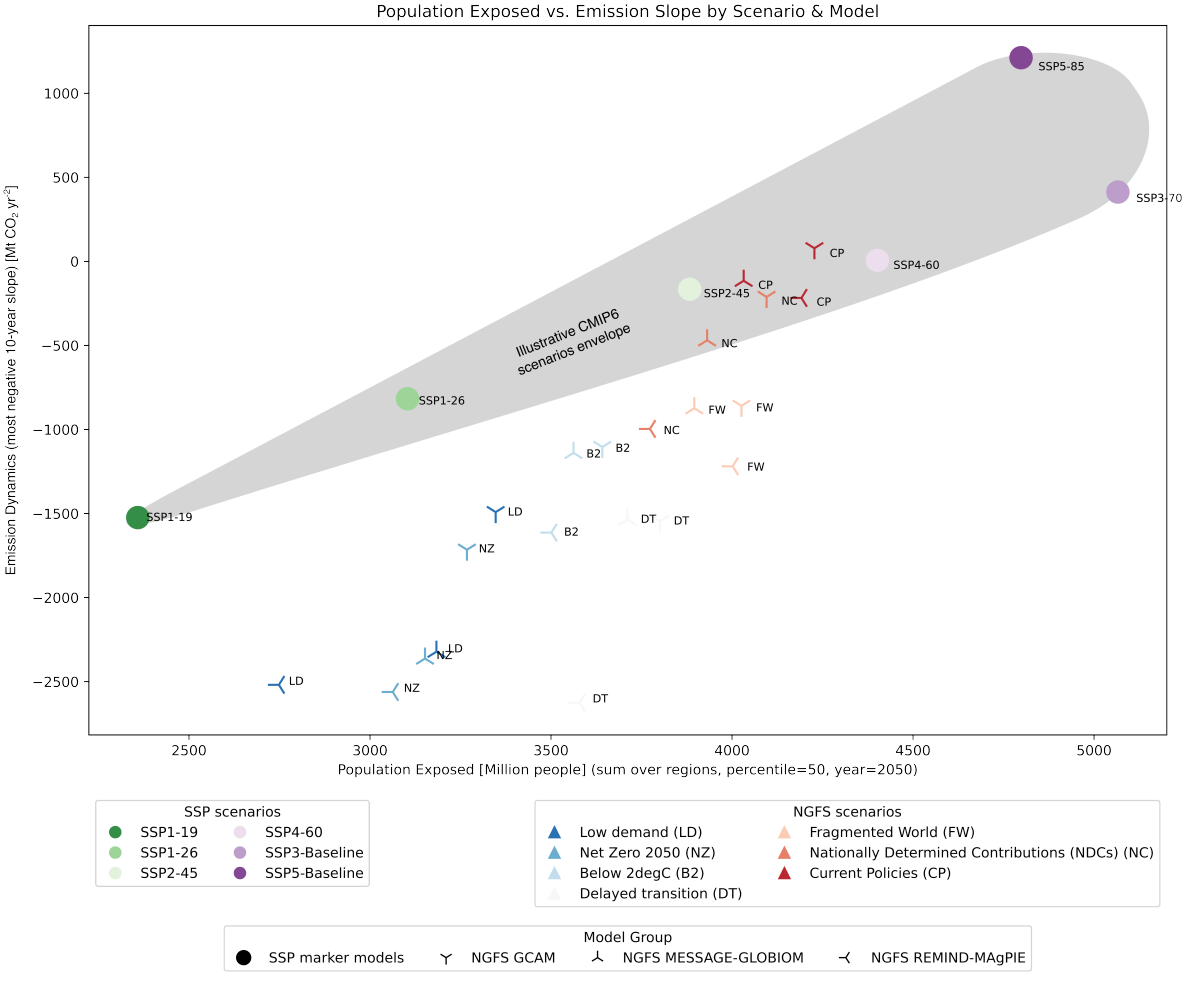

Figure 3. Global aggregate of spatial scenario-to-climate outcomes for CMIP6 and NGFS scenarios. Scenarios are positioned in an emissions-climate outcome space defined by emission pathway dynamics (y-axis: most negative 10-year slope in net CO_2 emissions up to 2050) and heat-exposure outcomes (x-axis: globally aggregated population exposed to annual maximum temperatures exceeding the preindustrial 97.5th percentile of TXx in 2050). Coloured symbols denote CMIP6 scenarios, triangles represent NGFS scenarios, and black outlines indicate CMIP6 scenario models. Population exposure only shows MESMER results emulated based on the median SCM projection. An illustrative envelope (grey) denotes the range covered by the CMIP6 scenarios.

https://doi.org/10.5194/egusphere-2026-2253
Preprint. Discussion started: 27 May 2026

Beyond extending the coverage, the quantitative positioning of scenarios using emulated outcomes helps interpret new scenarios relative to well-studied reference cases. For instance, the NGFS Current Policies scenario falls between SSP2-45 and SSP4-60 in terms of both emission pathway dynamic and heat-exposure outcome. This positioning suggests that existing literature on these SSPs may provide useful analogues when interpreting Current Policies results. In contrast, the most ambitious NGFS scenarios (Net Zero 2050 and Low Demand) are located further away from the SSP1-19 and SSP1-26 scenarios, indicating combinations of emissions trajectories and climate outcomes that are not well represented by previous CMIP6 scenarios and therefore could benefit from an assessment that compares differences between these scenarios.

Spatial emulation thus enables a systematic quantification of the broader scenario-to-climate outcome space. By enabling the translation of more diverse socioeconomic pathways into spatially explicit climate outcomes, spatial emulation can reveal gaps in current scenario coverage and identify where future modelling efforts could most effectively expand coverage.

3.3 Assessing previously unexplored regional heterogeneity

Global, aggregated assessments of climate outcomes can hide their underlying regional variation. Spatial emulators can help reveal this spatial heterogeneity, e.g. by enabling the assessment of country-specific climate outcomes directly linked to socioeconomic scenarios.

Under the NGFS Nationally Determined Contributions (NDCs) scenario, countries differ markedly in how their mitigation efforts (in per-capita emissions trajectories) relate to their population exposure to heat extremes (TXx exceeding the pre-industrial 97.5th percentile) between 2020 and 2050 (Figure 4). Countries such as Ethiopia and Spain are projected to experience much higher mid-century population exposure despite relatively low per-capita emissions compared to the global average with the two starting from markedly different conditions in 2020. Other countries, such as China and Thailand, combine higher per-capita emissions with relatively low population exposure compared to the global average.

This regional heterogeneity illustrates how global-mean results can mask pronounced regional contrasts, thus informing regional inequalities. For example, regions with high exposure but limited emissions contributions may face adaptation pressures that are disproportionate to their role in driving global change, reinforcing the inequalities related to climate change. Conversely, regions combining high emissions with high exposure may experience simultaneous mitigation and adaptation challenges. The availability of spatially explicit outcomes helps to contextualize these differences, providing information that can support impact and adaptation assessments at a much more actionable spatial scale.

https://doi.org/10.5194/egusphere-2026-2253
Preprint. Discussion started: 27 May 2026

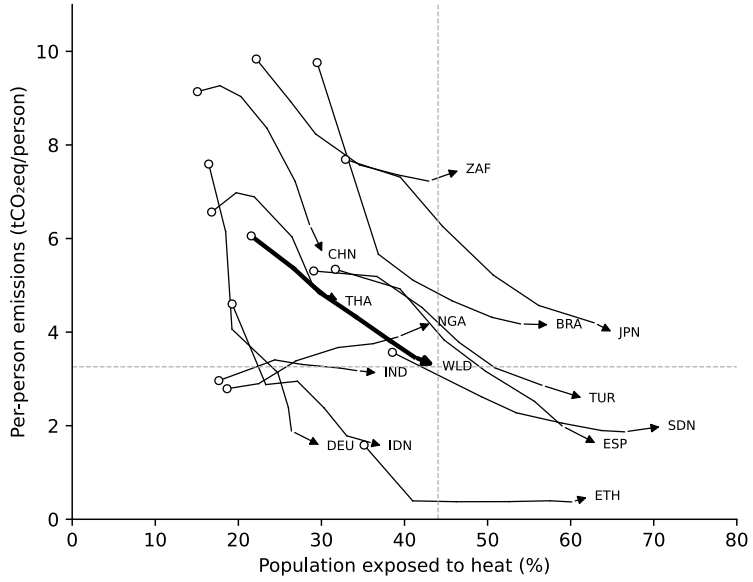

Country	ΔE	ΔP
NGA	+1.4	+25
IND	+0.2	+19
ETH	-1.1	+27
SDN	-1.6	+33
THA	-1.9	+16
ZAF	-2.4	+25
TUR	-2.7	+33
WLD	**-2.8**	**+22**
IDN	-3.0	+18
CHN	-3.5	+15
JPN	-3.7	+32
ESP	-3.8	+32
BRA	-5.6	+28
DEU	-6.0	+14

Figure 4. (a) Population share exposed to heat (exceeding the preindustrial 97.5th percentile of TXx) versus per-capita emissions for selected countries from 2020 (circle) to 2050 (arrow) under the NGFS' Nationally Determined Contributions (NDCs) scenario. The dashed line marks the 2050 global average. (b) Changes in per-capita emissions (ΔE, tCO_2eq/person) and heat-exposed population share (ΔP, percentage points), sorted by decreasing ΔE. Country codes follow ISO3 standards: Ethiopia (ETH), Japan (JPN), Turkey (TUR), Spain (ESP), Germany (DEU), Sudan (SDN), China (CHN), Brazil (BRA), Nigeria (NGA), India (IND), Indonesia (IDN), South Africa (ZAF), Thailand (THA), World (WLD).

However, the exposure of the population to the hazard (heat extremes) computed by the spatial emulator does not yet represent risk. Translating climate extremes into risk requires considering vulnerability, the degree to which populations, sectors, or ecosystems are sensitive to climatic stress. The example in Figure 4 therefore captures only one component of the countries' risk of heat extremes: the physical hazard and the spatial coincidence of exposed populations. Further progress will require coupling emulated climate information with data that represent vulnerability dimensions such as outdoor labour intensity, income distribution, or demographic structure.

Current spatial emulators provide fields of temperature, precipitation, or derived indices (e.g., TXx, drought frequency, or degree-day metrics), but they do not account for how socioeconomic and biophysical vulnerability modulate impacts. Integrating emulated climate outcomes with sector-specific exposure and vulnerability data could allow for a more comprehensive representations of risk, for instance, by linking crop-specific yield sensitivities to heat or identifying labour sectors where exposure to high wet-bulb temperatures constrains productivity.

In this sense, the emulator framework only offers a foundation for more comprehensive regional risk assessments. Its strength lies in providing rapid, spatially explicit, and probabilistic physical inputs for a much broader set of future scenarios that can be combined with existing or emerging vulnerability datasets. As such, emulators can help identify, societal

https://doi.org/10.5194/egusphere-2026-2253
Preprint. Discussion started: 27 May 2026

developments, regions or socioeconomic groups that warrant more detailed study, and support the prioritization of adaptation strategies.

3.4 Exploring previously unquantified scenario outcomes

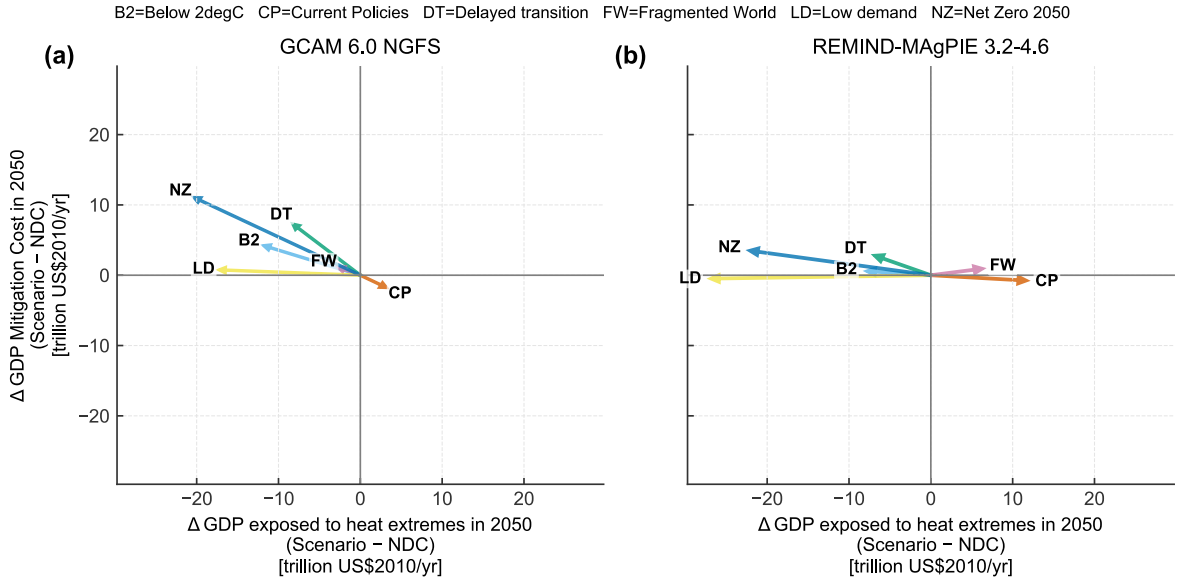

Figure 5. Comparison of 2050 GDP-related mitigation cost and heat exposure across NGFS scenarios for two IAMs (GCAM 6.0 and REMIND–MAgPIE 3.2–4.6). The x-axis shows the difference in exposed GDP relative to the NDC scenario, and the y-axis shows the difference in mitigation costs both for the year 2050. Negative values on the x-axis indicate lower economic exposure to heat extremes, while negative values on the y-axis represent lower mitigation costs compared to the NDCs scenario.

By extending spatial climate information to a broader range of socioeconomic scenarios, spatial emulation enables the quantification of scenario outcomes that were previously unquantified at a spatially specific scale. This includes trade-offs between mitigation expenditures and spatially explicit avoided economic exposure to climate extremes.

To evaluate this trade-off, we combine country-specific, IAM-based socioeconomic information with emulator-based spatial climate outcomes (Figure 5). Expressed relative to the NDCs baseline and summarized here as global aggregates, the results reveal substantial variation in how efficiently scenarios translate mitigation expenditures into avoided economic exposure. These spatially explicit NGFS scenario outcomes, and by extension most other climate outcomes of societal developments explored by IAM scenarios, would remain unexplored without emulators extending the scenario-to-climate space.

The analysis of country-level GDP heat exposure reveals substantial variation in the economic efficiency of mitigation across scenarios. For example, the Current Policies scenario reduces mitigation costs relative to the NDCs by approximately –1.8 trillion USD/yr in GCAM and –0.8 trillion USD/yr in REMIND–MAgPIE but increases the exposure of economic activity to heat extremes by +3.3 and +11.8 trillion USD/yr, respectively. By contrast, the two most ambitious mitigation pathways, Net Zero 2050 and Low Demand, both reduce the GDP exposed to heat extremes by similar magnitudes (–20.4 / –

https://doi.org/10.5194/egusphere-2026-2253
Preprint. Discussion started: 27 May 2026

17.4 trillion USD/yr in GCAM; –22.3 / –27.0 trillion USD/yr in REMIND–MAgPIE), while Low Demand incurs much smaller or even negative differences in mitigation costs. In GCAM, Low Demand is only slightly more costly than merely achieving the NDCs (+0.8 trillion USD/yr) but achieves reductions in exposure (–17.4 trillion USD/yr) comparable to Net Zero 2050; in REMIND–MAgPIE, the Low Demand scenario is in fact less costly than the NDCs (–0.5 trillion USD/yr) while avoiding –27 trillion USD/yr in exposed GDP.

These results demonstrate how spatial emulation allows for a first quantitative exploration of efficiency trade-offs between mitigation expenditures and avoided physical exposure for scenarios without dedicated ESM runs. Such comparisons were previously infeasible because ESM-based regional outcomes are available only for a limited subset of scenarios. With emulator-generated climate data, this type of analysis can be extended systematically across a wide range of socioeconomic futures.

However, as in the previous sections, the interpretation of such regional results again depends on the availability of regional (or country-specific) socioeconomic output data of IAMs. Again, the exposed GDP is also only a partial indicator of risk. It measures the economic value located in areas projected to experience heat extremes but does not account for local vulnerability, adaptive capacity, or sector-specific sensitivities. A dollar of exposed GDP in a high-income economy may be at a smaller actual risk than the same exposure in a lower-income or climate-sensitive region. Further integration of vulnerability indicators, such as sectoral composition, labour exposure, or access to cooling, would be required to interpret these values in terms of economic risk.

4 Drivers of uncertainty in emulated regional climate outcomes

While spatial emulators enable probabilistic regional projections, the resulting uncertainty depends on both emulator design choices (is the emulator emulating different ESMs, and how many?; is the emulator representing internal variability?) and the experimental setup defining the input data used to generate the projections (how is the probabilistic representation of the global temperature mean response achieved by the SCMs? What range of percentiles is used to span such uncertainty range?). These differences are illustrated by comparing emulated temperature responses for an example region and scenario, here Western Africa under the NGFS Current Policies scenario, across the three participating spatial emulators (Figure 6, figures for all AR6 regions are available on Zenodo).

The comparison highlights how emulator and experiment design influences both the amplitude and structure of regional uncertainty. PRIME produces smooth trajectories because it does not include interannual variability. STITCHES, by contrast, reproduces the interannual variability of the ESMs it emulates but in this experimental setup only provided a smaller emulated pool (eight ESMs), leading to a narrower spread. MESMER, emulated a larger set of ESMs (54 ESMs), yielding both a broader cross-ESMs spread like PRIME but including interannual variability like STITCHES.

The decomposition of spread (Figure 6, right-hand panels) clarifies how different characteristics shape the total uncertainty envelope. In MESMER and PRIME, the larger number of emulated ESMs broadens the inter-model range in comparison to

https://doi.org/10.5194/egusphere-2026-2253
Preprint. Discussion started: 27 May 2026

STITCHES (boxes), while PRIME's smooth projections dampen temporal spread (violins). This reflects the fact that, in the configuration used here, PRIME represents only the forced response and does not include internal variability. Consequently, PRIME cannot capture the tails of the distribution arising from the combination of forced response and internal variability. These differences demonstrate that the relative contribution of uncertainty sources from driving SCM percentile inputs, emulated ESM diversity, and interannual variability, depends both on emulator design and experimental design. The SCM percentile range, representing the global mean temperature response to climate forcing probabilistically quantified, dominates the central tendency and overall warming range, while emulator architecture and training diversity determines the spread at regional scales.

These design differences affect the tails of the temperature distribution emulated for Western Africa. MESMER emulations exceed 5 K of warming in 12 % of yearly values when it is driven by the trajectory of global mean temperature that corresponds to the 95th percentile of the SCM probabilistic ensemble output and in 2 % when driven by the 90th percentile of the SCM ensemble, whereas PRIME and STITCHES only exceed 5 K of warming in Western Africa in 3 % and 1 % of their emulations despite being driven by the same 95th percentile of the SCM ensemble, respectively, and none when driven by the 90th percentile. When aggregated to decadal means (2090–2099), MESMER produces seven emulated ESMs with warming above 5 K when driven by the 95% of the SCM ensemble (7 of 54; ≈ 13 %), PRIME produces one (1 of 33; ≈ 3 %), and STITCHES produces none.

Central estimates remain more consistent across emulators. The inter-ESM median difference in near surface air temperature Δtas for Western Africa in the 2090s based on the 50th percentile of the SCM ensemble is 3.01 K for MESMER, 2.87 K for STITCHES, and 2.83 K for PRIME, with late-century decadal medians based on the 5th-95th percentile SCM input spanning 2.18–4.29 K (MESMER), 2.00–4.02 K (STITCHES), and 2.07–4.12 K (PRIME).

Together this underscores that while emulators generate regional probabilistic climate outcomes, their treatment of variability and uncertainty introduced by structural characteristics, experiment design and training data requires careful interpretation, particularly when analyses are based on single emulators or when outcomes of different emulators and experimental setup are intercompared. A multi-emulator ensemble can provide a more comprehensive picture of uncertainty across the scenario-to-climate chain.

https://doi.org/10.5194/egusphere-2026-2253
Preprint. Discussion started: 27 May 2026

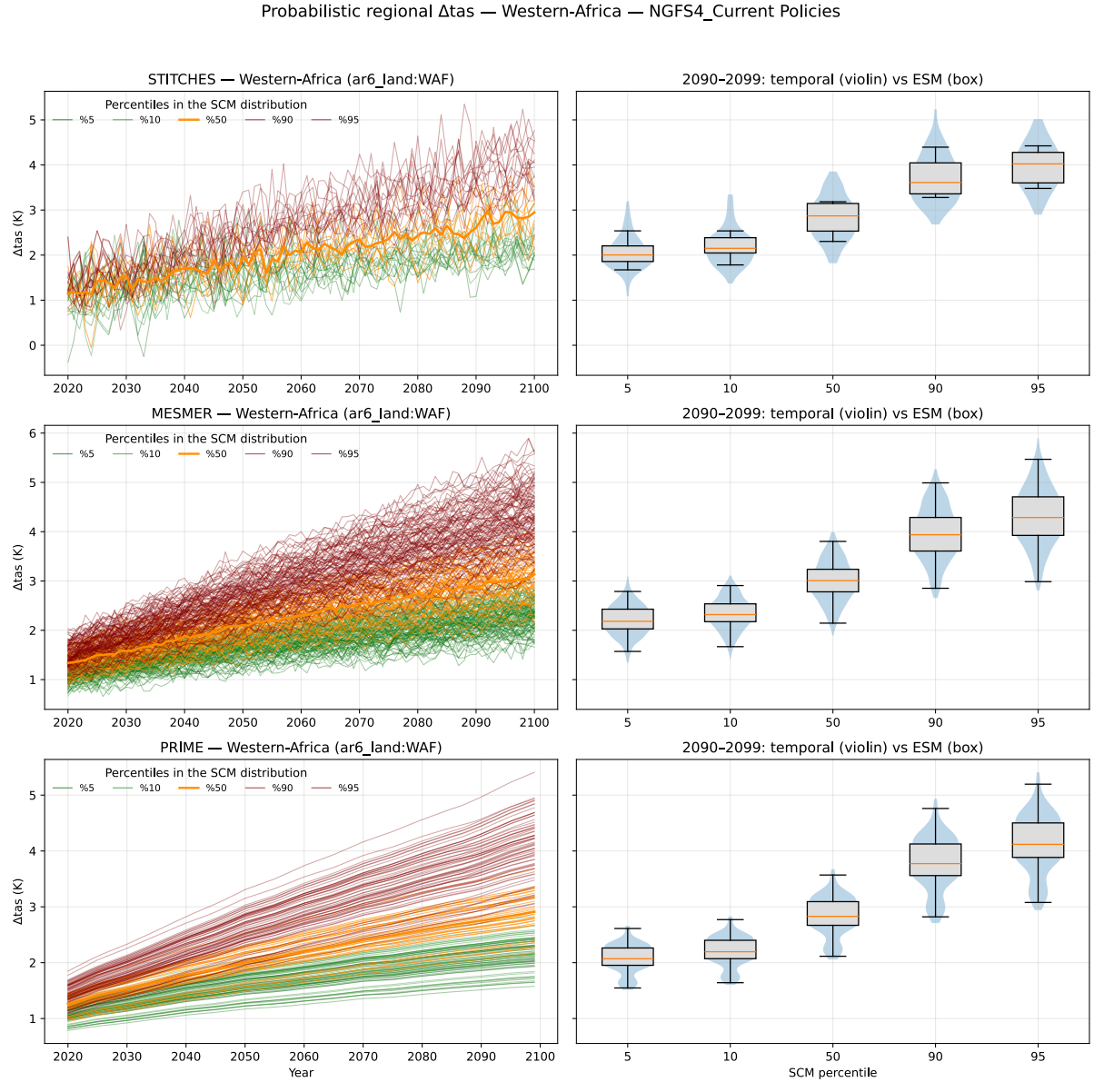

Figure 6. Probabilistic regional temperature change for Western Africa under the NGFS Current Policies scenario. Anomalies are relative to each emulator's historical 1850–1900 mean. Monthly outputs are averaged to annual values. The SCM forcing is provided as five percentiles (5, 10, 50, 90, 95) of the global temperature response. Left panels: time evolution of near surface air temperature (Δtas) for 2020–2100, with thin coloured lines showing per-ESM emulated temperatures for each SCM percentile; the bold orange line highlights the cross-ESM median at the 50th percentile. Right panels: decomposition of 2090–2099 uncertainty by SCM percentile, where violins depict temporal (interannual) variability from all annual values pooled across members, and boxplots summarize spread across emulated ESMs using the decadal mean per ESM. Both temporal and emulated ESM spread are provided for the five SCM percentiles.

https://doi.org/10.5194/egusphere-2026-2253
Preprint. Discussion started: 27 May 2026

5 Conclusions

This study introduces the FASTMIP pilot experiment, demonstrating how spatial climate emulators can operationalize a faster and more comprehensive connection between socioeconomic scenarios and regional climate outcomes, extending spatial information to the dominant share of IAM scenarios currently not covered by dedicated ESM simulations.

The coordinated experiment illustrates four key opportunities of spatial emulators.

First, spatial emulation provides a starting point for representing feedback between scenarios and their climate outcomes by making spatially explicit climate information available more rapidly and widely across scenarios. In principle, such information could be used to endogenously constrain scenario assumptions, for example by identifying where land-based mitigation measures become less plausible under projected regional climate conditions. As an illustration of this potential, we demonstrate how an emulator-derived fire-weather indicator can be combined with the land-use patterns from IAMs to identify planned forested areas exposed to elevated future fire-weather risk. The fire exposure evaluation provides an initial example of how emulated spatial climate information could inform constraints on land-based mitigation options by identifying regions where reforestation may be compromised by climate-driven hazards. While this demonstration does not yet translate hazards into expected carbon losses within the IAM's cost-optimized mitigation pathway, it illustrates how spatially explicit climate information can reveal feedback affecting emission pathways and motivate the exploration of alternative, more robust scenario variants.

Second, emulated outcomes allow a more complete mapping of the scenario-to-climate space and can position new or exploratory scenarios relative to established pathways, highlighting where additional simulations would most effectively extend coverage. Third, spatial emulation provides regional and country-scale perspectives on future climate outcomes that can inform impact and adaptation assessments at more actionable spatial scales than a global value. Such regional climate information is essential for the analysis of inequalities in climate impacts.

Fourth, the emulator output supports the quantification of outcomes that are otherwise inaccessible for scenarios without ESM, such as trade-offs between mitigation costs and avoided physical exposure of country-based economic activity to heat extremes.

However, currently these assessments are still limited and require advances on both sides of the scenario-to-climate interface. Translating hazards into impacts affecting socio-economic pathways in IAMs is a challenging research and modelling direction, and IAMs have limited capacity to ingest gridded climate information directly into their socioeconomic constraints. More readily interpretable inputs such as country-level aggregates and/or spatially masked indicators (e.g., regions unsuitable for reforestation under high fire-weather risk) could facilitate the exchange between spatial emulation and scenario development. Similarly, the restricted spatial detail of many publicly available IAM outputs constrains exogenous analyses. More disaggregated information on the location of populations, assets, and land uses, as well as on sectoral or demographic composition, would enable more meaningful connections between climate exposure, hazard, and vulnerability,

https://doi.org/10.5194/egusphere-2026-2253
Preprint. Discussion started: 27 May 2026

thereby supporting more comprehensive risk and impact assessments in the global perspective afforded by these modelling tools.

The experiment also underscores the importance of understanding uncertainty within the emulator framework. Differences in emulator design, training data, and input configuration influence how variability and structural uncertainty are represented so results should always be interpreted with the emulator design and input configuration in mind. Coordinated multi-emulator ensembles therefore could offer a practical way to capture and interpret assumption and setup-based uncertainty across the scenario-to-climate chain.

Spatial emulation offers a path to provide regional climate information faster and for a much broader set of socioeconomic scenarios than current CMIP-type efforts, enabling systematic comparison between them by trading process detail for computational efficiency. Further, they provide a promising starting point towards iterative exchange between socioeconomic projections and climate feedback. Applying a similar coordinated multi-emulator approach in upcoming ScenarioMIP exercises could translate this capability into earlier regional insights, including extremes and carbon cycle feedback (Varney et al., 2025), and support the development of more consistent and robust scenario assumptions and climate outcomes.

6 Methods

6.1 FASTMIP pilot experiment design

This study presents the FASTMIP pilot experiment, a coordinated experiment with spatial climate emulators aimed to rapidly translate socioeconomic scenarios into spatial climate outcomes. The FASTMIP pilot coordinates three spatial emulators using shared forcing inputs from Simple Climate Models (SCMs). These scenario inputs used in the FASTMIP pilot experiment are publicly available from the IIASA Scenario Explorer Database and the FASTMIP ETH data archive. All resulting emulator outputs are archived to enable other emulators to reproduce the experiment and compare results. The following sections describe the selected scenarios, forcing data, participating emulators, and generated output variables of the FASTMIP pilot experiment.

6.2 Scenarios

Three groups of scenarios were analysed. The first group comprises the tier 1 SSP–RCP scenarios SSP1-1.9, SSP1-2.6, SSP2-4.5, SSP3-7.0, and SSP5-8.5 (here termed CMIP6 scenarios). The second group consists of seven scenarios from the Network for Greening the Financial System (NGFS), namely Net Zero 2050, Low Demand, Below 2°C, Delayed Transition, NDCs, Current Policies, and Fragmented World. The third group includes scenarios from recent EU projects (PROVIDE and RESCUE), focusing on overshoot pathways, carbon dioxide removal, and specific cases such as SSP5-3.4-OS, World Bank 2°C and 1.5°C scenarios with and without overshoot, GS_NZGHG, and NEG_OS_0. Several of these scenarios, including

https://doi.org/10.5194/egusphere-2026-2253
Preprint. Discussion started: 27 May 2026

the tier 1 CMIP6 scenarios and SSP5-3.4-OS, are also available from full ESM experiments, allowing for direct comparison while the second group of scenarios (NGFS) were not run by ESMs .

6.3 Forcing data and probability levels

The scenarios were driven by outputs from Simple Climate Models (SCMs) based on emission scenarios of Integrated Assessment Models (IAMs). For each scenario–SCM combination, probabilistic realizations of global mean temperature (GMT) change were used at the 5th, 10th, 50th, 90th, and 95th percentiles in their distribution, which is a function of parametric uncertainty (taking into account, for example, the IPCC AR6 assessment of the distribution of equilibrium climate sensitivity) and observational constraints (Smith et al., 2024). The IAM and SCM outputs used here were sourced from the IIASA Scenario Explorer Database (Byers et al., 2022.). The IAM and SCM model versions and types differ across experiments.

6.4 Emulators

Spatial climate projections were generated using three spatial climate emulators trained on CMIP6 Earth System Models: MESMER, PRIME, and STITCHES. MESMER emulated 54 CMIP6 ESMs, PRIME emulated 33 ESMs, and STITCHES emulated 8 ESMs. The full list of emulated ESMs for each emulator is shown in Table 1. All three emulators were forced with identical SCM-derived global mean temperature trajectories at the five SCM percentiles specified in the forcing data section to ensure comparability across emulators.

Table 1. Emulated ESMs by emulator. List of Earth System Models emulated by each emulator (MESMER, PRIME, STITCHES), summarizing the model coverage of the emulation ensemble.

https://doi.org/10.5194/egusphere-2026-2253
Preprint. Discussion started: 27 May 2026

MESMER 1/2	MESMER 2/2	STITCHES	PRIME
ACCESS-CM2	GISS-E2-2-G	ACCESS-ESM1-5	ACCESS-CM2
ACCESS-ESM1-5	HadGEM3-GC31-LL	CMCC-CM2-SR5	ACCESS-ESM1-5
AWI-CM-1-1-MR	HadGEM3-GC31-MM	CanESM5	AWI-CM-1-1-MR
BCC-CSM2-MR	INM-CM4-8	MIROC-ES2L	BCC-CSM2-MR
CAMS-CSM1-0	INM-CM5-0	MIROC6	CMCC-ESM2
CAS-ESM2-0	IPSL-CM5A2-INCA	MPI-ESM1-2-HR	CNRM-CM6-1
CESM2	IPSL-CM6A-LR	MPI-ESM1-2-LR	CNRM-CM6-1-HR
CESM2-FV2	KACE-1-0-G	MRI-ESM2-0	CNRM-ESM2-1
CESM2-WACCM	MCM-UA-1-0		CanESM5
CIESM	MIROC-ES2H		CanESM5-1
CMCC-CM2-SR5	MIROC-ES2L		CanESM5-CanOE
CMCC-ESM2	MIROC6		EC-Earth3
CNRM-CM6-1	MPI-ESM1-2-HR		EC-Earth3-Veg
CNRM-CM6-1-HR	MPI-ESM1-2-LR		FGOALS-g3
CNRM-ESM2-1	MRI-ESM2-0		GFDL-CM4
CanESM5	NESM3		GFDL-ESM4
CanESM5-1	NorESM2-LM		GISS-E2-1-G
CanESM5-CanOE	NorESM2-MM		GISS-E2-1-H
E3SM-1-1	TaiESM1		GISS-E2-2-G
E3SM-1-1-ECA	UKESM1-0-LL		HadGEM3-GC31-LL
E3SM-2-0	UKESM1-1-LL		HadGEM3-GC31-MM
EC-Earth3			INM-CM4-8
EC-Earth3-AerChem			INM-CM5-0
EC-Earth3-CC			IPSL-CM6A-LR
EC-Earth3-Veg			MIROC-ES2H
EC-Earth3-Veg-LR			MIROC-ES2L
FGOALS-f3-L			MIROC6
FGOALS-g3			MPI-ESM1-2-HR
FIO-ESM-2-0			MPI-ESM1-2-LR
GFDL-CM4			MRI-ESM2-0
GFDL-ESM4			NorESM2-MM
GISS-E2-1-G			TaiESM1
GISS-E2-1-H			UKESM1-0-LL

6.4.1 PRIME

This analysis uses part of the PRIME (Probabilistic Regional Impacts from Model patterns and Emissions) modelling framework (Mathison et al., 2025). PRIME usually starts from emissions and uses the FaIR simple climate model to convert

https://doi.org/10.5194/egusphere-2026-2253
Preprint. Discussion started: 27 May 2026

these to a temperature and CO2 concentration, however it can also ingest global mean temperatures directly and produce spatially resolved climate outputs in a similar way to MESMER using linear pattern scaling, which is the approach used in this analysis. Global temperatures were provided for each scenario and used to scale the CMIP6 patterns, which were generated using ESMValTool recipe (Andela et al., 2024.). In the standard PRIME set up, these climate patterns would then be downscaled to provide hourly driving data to run the JULES land surface model and derive land impacts for a wide range of variables, but this part of the framework has not been run in this analysis.

6.4.2 STITCHES

STITCHES (Snyder et al., 2024; Tebaldi et al., 2022) is a climate emulator that can produce time series of multiple ESM variables, at the ESM original temporal and spatial resolution, by recombining existing model output into new scenarios on the basis of the scenario's global temperature trajectory. It can be viewed as the extension of the concept of time sampling – usually applied to individual global warming levels – to a full 21st century trajectory of global average temperature. By subsampling and connecting pre-existing segments (usually ~10-years long) of ESM experiments according to their global temperature behaviour, STITCHES preserves the ESM variability, and consistency among variables. However, it is limited by the availability of existing experiments from which to sample both in terms of the number of realizations and in terms of the type of experiment it can produce. For example, it may fail to emulate a new scenario with a strong temperature overshoot, if the ESM has never run overshoot experiments from which to subsample. It would be also inappropriate for the emulation of path-dependent, long memory (beyond ~10 years) variables, mega-drought or sea level rise being primary examples. In the mega-drought case, splitting existing experiments into 10-year segments as the building blocks to be recombined would likely break the coherence of a long-lasting episode. In the sea level rise case, using instantaneous global temperature as the sole look-up index would not account for the fact that sea level rise is an integrator of the entire past trajectory of global temperature. However, the majority of atmospheric variables that are usually targeted by emulators because of their relevance as climatic impact drivers can be considered as having short-memory and not path dependent.

6.4.3 MESMER

MESMER is a spatially resolved climate emulator that mimics the response of ESMs to changes in global mean surface temperature. This emulator is calibrated on CMIP6 data to replicate both the mean response and the natural variability for every ESM, thus allowing the analysis of model uncertainties. For FASTMIP, the following climate indicators were produced as follows, each using global mean surface temperatures from the SCM as inputs. Annual mean temperatures were deduced from pattern scaling for the mean response and local auto-regressive processes with spatially correlated innovations to represent natural variability (Beusch et al., 2020). Monthly temperatures were obtained by using local harmonic models for the forced response, and the natural variability uses the same elements but in a transformed Gaussian space thanks to Yeo-Johnson power transformation (Nath et al., 2022). Other variables related to temperatures (annual maximum temperatures), soil moisture (annual average, annual minimum of the monthly average) and fire weather (annual maximum,

https://doi.org/10.5194/egusphere-2026-2253
Preprint. Discussion started: 27 May 2026

annual average over fire season, length of the fire season, number of days with extreme fire weather) are derived from local conditional distributions for the probabilistic response, and the natural variability is inferred from local auto-regressive processes with spatially correlated innovations in a transformed Gaussian space using a probability integral transform(Quilcaille et al., 2022, 2023). All outputs of MESMER (variables, scenarios, percentiles of SCMs) were archived both using 10 random emulations and a set of 11 percentiles based on 1000 emulations.

6.5 Output specifications

All outputs extend to the year 2100 and are harmonized to a common 2.5° by 2.5° latitude–longitude grid to facilitate comparisons. Annual data were produced for all simulations, and monthly data were generated where available (Table 2.). The core set of variables emulated by all three emulators includes annual mean surface temperature (computed from monthly values in the case of PRIME) and precipitation. Additional variables are produced flexibly, depending on emulator capabilities, e.g. covering climate extremes such as annual maximum temperature and daily maximum precipitation, water cycle components such as soil moisture, and specific humidity.

Each emulated ESM–SCM–scenario combination was represented by one core realization. In addition, up to ten realizations with interannual variability were permitted. Each realization also carries an emulation, depending on the scenario, for each individual IAM, SCM, and SCM percentile.

Table 2. Emulated variables. Overview of available variables by temporal resolution (annual "ann" & monthly "mon") and emulator (MESMER, PRIME, STITCHES); an "X" indicates that the corresponding emulator provides output for the given variable and frequency.

variable	ann_MESMER	ann_PRIME	ann_STITCHES	mon_MESMER	mon_PRIME	mon_STITCHES
fwils	X					
fwisa	X					
fwixd	X					
fwixx	X					
huss					X	
mrso	X					
mrso_minmon	X					
pr					X	X
ps					X	
range_tl1					X	
rlds					X	
rsds					X	
sfcWind					X	
tas	X		X		X	X
txx	X					

https://doi.org/10.5194/egusphere-2026-2253
Preprint. Discussion started: 27 May 2026

Code and data availability

All spatially emulated climate outputs generated by the three emulators (MESMER, PRIME, and STITCHES) are available by FTP server hosted at ETH Zurich for the review and will be made publicly available from the ETH Research Collection. Code and post-processed data specific to the assessments here are available at Zenodo (https://doi.org/10.5281/zenodo.19603331).

Author contributions

M.G.W, Y.Q, C.M., C.T., E.B, L.G, C.S, and S.I.S conceived the study which was further refined by S.S, A.S, S.D., and K.D.

M.G.W, Y.Q, C.M., C.T., E.B, L.G, C.S, A.S, S.D., and K.D performed the emulations.

M.G.W. drafted the manuscript and created the figures with significant input from all co-authors.

Competing interests

At least one of the (co-)authors is a member of the editorial board of Earth System Dynamics.

Acknowledgements

We thank Marthin Hirschi, Mathias Hauser, and Urs Beyerle for their technical support in setting up and maintaining the data infrastructure, including storage and data access workflows.

This work was supported by funding from the European Union's Horizon 2020 Research and Innovation Programme under grant agreement number 101056939 (RESCUE). C.T., A.S, S.D., and K.D are also affiliated with the Pacific Northwest National Laboratory, which did not provide specific support for this work. CM, EJB and LKG were supported by the Met Office Hadley Centre Climate Programme funded by DSIT.

References

Andela, B., Broetz, B., de Mora, L., Drost, N., Eyring, V., Koldunov, N., Lauer, A., Mueller, B., Predoi, V., Righi, M., Schlund, M., Vegas-Regidor, J., Zimmermann, K., Adeniyi, K., Arnone, E., Bellprat, O., Berg, P., Bock, L., Bodas-Salcedo, A., Caron, L.-P., Carvalhais, N., Cionni, I., Cortesi, N., Corti, S., Crezee, B., Davin, E. L., Davini, P., Deser, C., Diblen, F., Docquier, D., Dreyer, L., Ehbrecht, C., Earnshaw, P., Gier, B., Gonzalez-Reviriego, N., Goodman, P., Hagemann, S., Hardacre, C., von Hardenberg, J., Hassler, B., Heuer, H., Hunter, A., Kadow, C., Kindermann, S., Koirala, S., Kuehbacher, B., Lledó, L., Lejeune, Q., Lembo, V., Little, B., Loosveldt-Tomas, S., Lorenz, R., Lovato, T., Lucarini, V., Massonnet, F.,

https://doi.org/10.5194/egusphere-2026-2253
Preprint. Discussion started: 27 May 2026

Mohr, C. W., Amarjiit, P., Pérez-Zanón, N., Phillips, A., Russell, J., Sandstad, M., Sellar, A., Senftleben, D., Serva, F., Sillmann, J., Stacke, T., Swaminathan, R., Torralba, V., Weigel, K., Sarauer, E., Roberts, C., Kalverla, P., Alidoost, S., Verhoeven, S., Vreede, B., Smeets, S., Soares Siqueira, A., Kazeroni, R., Potter, J., Winterstein, F., Beucher, R., Kraft, J., Ruhe, L., Bonnet, P., and Munday, G.: ESMValTool, https://doi.org/10.5281/ZENODO.12654299, 2024.

Beusch, L., Gudmundsson, L., and Seneviratne, S. I.: Emulating Earth system model temperatures with MESMER: From global mean temperature trajectories to grid-point-level realizations on land, Earth System Dynamics, 11, 139–159, https://doi.org/10.5194/ESD-11-139-2020, 2020.

Byers, E., Krey, V., Kriegler, E., Riahi, K., Schaeffer, R., Kikstra, J., Lamboll, R., Nicholls, Z., Sandstad, M., Smith, C., van der Wijst, K., Al -Khourdajie, A., Lecocq, F., Portugal-Pereira, J., Saheb, Y., Stromman, A., Winkler, H., Auer, C., Brutschin, E., Gidden, M., Hackstock, P., Harmsen, M., Huppmann, D., Kolp, P., Lepault, C., Lewis, J., Marangoni, G., Müller-Casseres, E., Skeie, R., Werning, M., Calvin, K., Forster, P., Guivarch, C., Hasegawa, T., Meinshausen, M., Peters, G., Rogelj, J., Samset, B., Steinberger, J., Tavoni, M., and van Vuuren, D.: AR6 Scenarios Database, https://doi.org/10.5281/ZENODO.7197970, 2022.

Calvin, K. and Bond-Lamberty, B.: Integrated human-earth system modelling—state of the science and future directions, Environmental Research Letters, 13, 063006, https://doi.org/10.1088/1748-9326/AAC642, 2018.

Collins, W. D., Craig, A. P., Truesdale, J. E., Di Vittorio, A. V., Jones, A. D., Bond-Lamberty, B., Calvin, K. V., Edmonds, J. A., Kim, S. H., Thomson, A. M., Patel, P., Zhou, Y., Mao, J., Shi, X., Thornton, P. E., Chini, L. P., and Hurtt, G. C.: The integrated Earth system model version 1: Formulation and functionality, Geosci. Model Dev., 8, 2203–2219, https://doi.org/10.5194/GMD-8-2203-2015, 2015.

Dasgupta, S., van Maanen, N., Gosling, S. N., Piontek, F., Otto, C., and Schleussner, C. F.: Effects of climate change on combined labour productivity and supply: an empirical, multi-model study, Lancet Planet. Health, 5, e455–e465, https://doi.org/10.1016/S2542-5196(21)00170-4/ATTACHMENT/F9ABD22F-AA15-40B1-A694-ACA36E0FA68F/MMC1.PDF, 2021.

Eyring, V., Bony, S., Meehl, G. A., Senior, C. A., Stevens, B., Stouffer, R. J., and Taylor, K. E.: Overview of the Coupled Model Intercomparison Project Phase 6 (CMIP6) experimental design and organization, Geosci. Model Dev, 9, https://doi.org/10.5194/gmd-9-1937-2016, 2016.

Hartin, C., Link, R., Patel, P., Mundra, A., Horowitz, R., Dorheim, K., and Clarke, L.: Integrated modelling of human-earth system interactions: An application of GCAM-fusion, Energy Econ., 103, 105566, https://doi.org/10.1016/J.ENECO.2021.105566, 2021.

Hejazi, M. I., Edmonds, J., Clarke, L., Kyle, P., Davies, E., Chaturvedi, V., Wise, M., Patel, P., Eom, J., and Calvin, K.: Integrated assessment of global water scarcity over the 21st century under multiple climate change mitigation policies, Hydrol. Earth Syst. Sci., 18, 2859–2883, https://doi.org/10.5194/HESS-18-2859-2014, 2014.

Hurtt, G. C., Chini, L. P., Frolking, S., Betts, R. A., Feddema, J., Fischer, G., Fisk, J. P., Hibbard, K., Houghton, R. A., Janetos, A., Jones, C. D., Kindermann, G., Kinoshita, T., Klein Goldewijk, K., Riahi, K., Shevliakova, E., Smith, S.,

https://doi.org/10.5194/egusphere-2026-2253
Preprint. Discussion started: 27 May 2026

Stehfest, E., Thomson, A., Thornton, P., van Vuuren, D. P., and Wang, Y. P.: Harmonization of land-use scenarios for the period 1500–2100: 600 years of global gridded annual land-use transitions, wood harvest, and resulting secondary lands, Clim. Change, 109, 117–161, https://doi.org/10.1007/s10584-011-0153-2, 2011.

Jäger, F., Schwaab, J., Quilcaille, Y., Windisch, M., Doelman, J., Frank, S., Gusti, M., Havlik, P., Humpenöder, F., Lessa Derci Augustynczik, A., Müller, C., Narayan, K. B., Padrón, R. S., Popp, A., van Vuuren, D., Wögerer, M., and Seneviratne, S. I.: Fire weather compromises forestation-reliant climate mitigation pathways, Earth System Dynamics, 15, 1055–1071, https://doi.org/10.5194/ESD-15-1055-2024, 2024.

Kikstra, J. S., Nicholls, Z. R. J., Smith, C. J., Lewis, J., Lamboll, R. D., Byers, E., Sandstad, M., Meinshausen, M., Gidden, M. J., Rogelj, J., Kriegler, E., Peters, G. P., Fuglestvedt, J. S., Skeie, R. B., Samset, B. H., Wienpahl, L., Van Vuuren, D. P., Van Der Wijst, K. I., Al Khourdajie, A., Forster, P. M., Reisinger, A., Schaeffer, R., and Riahi, K.: The IPCC Sixth Assessment Report WGIII climate assessment of mitigation pathways: from emissions to global temperatures, Geosci. Model Dev., 15, 9075–9109, https://doi.org/10.5194/GMD-15-9075-2022, 2022.

Mathison, C., Burke, E. J., Munday, G., Jones, C. D., Smith, C. J., Steinert, N. J., Wiltshire, A. J., Huntingford, C., Kovacs, E., Gohar, L. K., Varney, R. M., and McNeall, D.: A rapid-application emissions-to-impacts tool for scenario assessment: Probabilistic Regional Impacts from Model patterns and Emissions (PRIME), Geosci. Model Dev., 18, 1785–1808, https://doi.org/10.5194/GMD-18-1785-2025, 2025.

Nath, S., Lejeune, Q., Beusch, L., Seneviratne, S. I., and Schleussner, C. F.: MESMER-M: an Earth system model emulator for spatially resolved monthly temperature, Earth System Dynamics, 13, 851–877, https://doi.org/10.5194/ESD-13-851-2022, 2022.

Popp, A., Calvin, K., Fujimori, S., Havlik, P., Humpenöder, F., Stehfest, E., Bodirsky, B. L., Dietrich, J. P., Doelmann, J. C., Gusti, M., Hasegawa, T., Kyle, P., Obersteiner, M., Tabeau, A., Takahashi, K., Valin, H., Waldhoff, S., Weindl, I., Wise, M., Kriegler, E., Lotze-Campen, H., Fricko, O., Riahi, K., and Vuuren, D. P. van: Land-use futures in the shared socio-economic pathways, Global Environmental Change, 42, 331–345, https://doi.org/10.1016/J.GLOENVCHA.2016.10.002, 2017.

Quilcaille, Y., Gudmundsson, L., Beusch, L., Hauser, M., and Seneviratne, S. I.: Showcasing MESMER-X: Spatially Resolved Emulation of Annual Maximum Temperatures of Earth System Models, Geophys. Res. Lett., 49, e2022GL099012, https://doi.org/10.1029/2022GL099012, 2022.

Quilcaille, Y., Gudmundsson, L., and Seneviratne, S. I.: Extending MESMER-X: a spatially resolved Earth system model emulator for fire weather and soil moisture, Earth System Dynamics, 14, 1333–1362, https://doi.org/10.5194/ESD-14-1333-2023, 2023.

Riahi, K., van Vuuren, D. P., Kriegler, E., Edmonds, J., O'Neill, B. C., Fujimori, S., Bauer, N., Calvin, K., Dellink, R., Fricko, O., Lutz, W., Popp, A., Cuaresma, J. C., KC, S., Leimbach, M., Jiang, L., Kram, T., Rao, S., Emmerling, J., Ebi, K., Hasegawa, T., Havlik, P., Humpenöder, F., Da Silva, L. A., Smith, S., Stehfest, E., Bosetti, V., Eom, J., Gernaat, D., Masui, T., Rogelj, J., Strefler, J., Drouet, L., Krey, V., Luderer, G., Harmsen, M., Takahashi, K., Baumstark, L., Doelman, J. C., Kainuma, M., Klimont, Z., Marangoni, G., Lotze-Campen, H., Obersteiner, M., Tabeau, A., and Tavoni, M.: The Shared

https://doi.org/10.5194/egusphere-2026-2253
Preprint. Discussion started: 27 May 2026

Socioeconomic Pathways and their energy, land use, and greenhouse gas emissions implications: An overview, Global Environmental Change, 42, 153–168, https://doi.org/10.1016/j.gloenvcha.2016.05.009, 2017.

Richters, O., Kriegler, E., Al Khourdajie, A., Bertram, C., Bresch, D. N., Ciullo, A., Cornforth, E., Cui, R., Edmonds, J., Fuchs, S., Hackstock, P., Holland, D., Hurst, I., Kikstra, J., Klein, D., Kotz, M., Kropf, C. M., Lewis, J., Liadze, I., Mandaroux, R., Meinshausen, M., Min, J., Nicholls, Z., Piontek, F., Sanchez Juanino, P., Sauer, I., Sferra, F., Stevanović, M., van Ruijven, B., Weigmann, P., Westphal, M. I., Zhao, A., and Zwerling, M.: NGFS Climate Scenarios Data Set, https://doi.org/10.5281/ZENODO.10807824, 2024.

Romero-Prieto, A., Mathison, C., and Smith, C.: Review of climate simulation by Simple Climate Models, Geosci. Model Dev., 19, 115–165, https://doi.org/10.5194/GMD-19-115-2026, 2026.

Schoenberg, W., Blanz, B., Rajah, J. K., Callegari, B., Wells, C., Breier, J., Grimeland, M. B., Lindqvist, A. N., Ramme, L., Smith, C., Li, C., Mashhadi, S., Muralidhar, A., and Mauritzen, C.: An overview of FRIDA v2.1: a feedback-based, fully coupled, global integrated assessment model of climate and humans, Geosci. Model Dev., 18, 8047–8069, https://doi.org/10.5194/GMD-18-8047-2025, 2025.

Smith, C., Cummins, D. P., Fredriksen, H. B., Nicholls, Z., Meinshausen, M., Allen, M., Jenkins, S., Leach, N., Mathison, C., and Partanen, A. I.: fair-calibrate v1.4.1: calibration, constraining, and validation of the FaIR simple climate model for reliable future climate projections, Geosci. Model Dev., 17, 8569–8592, https://doi.org/10.5194/GMD-17-8569-2024, 2024.

Smith, C. J. and Gasser, T.: Modelling the non-CO2 contribution to climate change, One Earth, 5, 1330–1335, https://doi.org/10.1016/j.oneear.2022.11.007, 2022.

Snyder, A. C., Dorheim, K. R., Tebaldi, C., and Vernon, C. R.: STITCHES: a Python package to amalgamate existing Earth system model output into new scenario realizations, J. Open Source Softw., 9, 5525, https://doi.org/10.21105/JOSS.05525, 2024.

Tebaldi, C., Debeire, K., Eyring, V., Fischer, E., Fyfe, J., Friedlingstein, P., Knutti, R., Lowe, J., O'Neill, B., Sanderson, B., Van Vuuren, D., Riahi, K., Meinshausen, M., Nicholls, Z., Tokarska, K., Hurtt, G., Kriegler, E., Meehl, G., Moss, R., Bauer, S., Boucher, O., Brovkin, V., Yhb, Y., Dix, M., Gualdi, S., Guo, H., John, J., Kharin, S., Kim, Y. H., Koshiro, T., Ma, L., Olivié, D., Panickal, S., Qiao, F., Rong, X., Rosenbloom, N., Schupfner, M., Séférian, R., Sellar, A., Semmler, T., Shi, X., Song, Z., Steger, C., Stouffer, R., Swart, N., Tachiiri, K., Tang, Q., Tatebe, H., Voldoire, A., Volodin, E., Wyser, K., Xin, X., Yang, S., Yu, Y., and Ziehn, T.: Climate model projections from the Scenario Model Intercomparison Project (ScenarioMIP) of CMIP6, Earth System Dynamics, 12, 253–293, https://doi.org/10.5194/ESD-12-253-2021, 2021.

Tebaldi, C., Snyder, A., and Dorheim, K.: STITCHES: creating new scenarios of climate model output by stitching together pieces of existing simulations, Earth System Dynamics, 13, 1557–1609, https://doi.org/10.5194/ESD-13-1557-2022, 2022.

Tebaldi, C., Selin, N. E., Ferrari, R., and Flierl, G.: Emulators of Climate Model Output, Annu. Rev. Environ. Resour., 50, 709–737, https://doi.org/10.1146/ANNUREV-ENVIRON-012125-085838, 2025.

https://doi.org/10.5194/egusphere-2026-2253
Preprint. Discussion started: 27 May 2026

Varney, R. M., Hooke, D., Steinert, N. J., Smallman, T. L., Mathison, C., and Burke, E. J.: Northern high latitudes could become a net carbon source below 2°C global warming, *EGUsphere* [preprint], https://doi.org/10.5194/egusphere-2025-6075, 2025.

Di Vittorio, A. V., Sinha, E., Hao, D., Singh, B., Calvin, K. V., Shippert, T., Patel, P., and Bond-Lamberty, B.: E3SM-GCAM: A Synchronously Coupled Human Component in the E3SM Earth System Model Enables Novel Human-Earth Feedback Research, J. Adv. Model. Earth Syst., 17, e2024MS004806, https://doi.org/10.1029/2024MS004806, 2025.

van Vuuren, D., O'Neill, B., Tebaldi, C., Chini, L., Friedlingstein, P., Hasegawa, T., Riahi, K., Sanderson, B., Govindasamy, B., Bauer, N., Eyring, V., Fall, C., Frieler, K., Gidden, M., Gohar, L., Jones, A., King, A., Knutti, R., Kriegler, E., Lawrence, P., Lennard, C., Lowe, J., Mathison, C., Mehmood, S., Prado, L., Zhang, Q., Rose, S., Ruane, A., Schleussner, C.-F., Seferian, R., Sillmann, J., Smith, C., Sörensson, A., Panickal, S., Tachiiri, K., Vaughan, N., Vishwanathan, S., Yokohata, T., and Ziehn, T.: The Scenario Model Intercomparison Project for CMIP7 (ScenarioMIP-CMIP7) , EGUsphere, 30, 1–38, https://doi.org/10.5194/EGUSPHERE-2024-3765, 2025.